

Plasmonic Optical Interferences for Phase-Monitored Nanoscale Sensing in Low-Loss Three-Dimensional Metamaterials

Johann Toudert,^{*,†,‡,§} Xuan Wang,^{†,‡} Clémence Tallet,^{†,‡} Philippe Barois,^{†,‡} Ashod Aradian,^{†,‡} and Virginie Ponsinet^{†,‡}

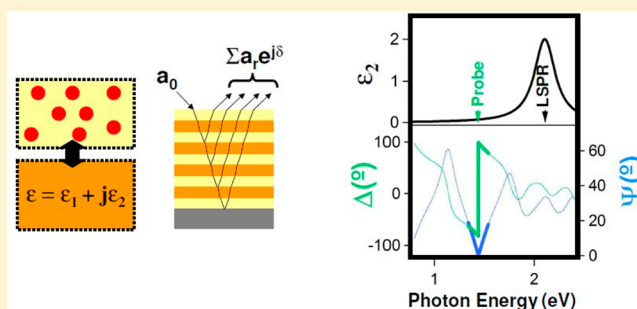
[†]CNRS, Centre de Recherche Paul Pascal UPR 8641, 115 Avenue Schweitzer, 33600 Pessac, France

[‡]Université de Bordeaux, Centre de Recherche Paul Pascal UPR 8641, 115 Avenue Schweitzer, 33600 Pessac, France

S Supporting Information

ABSTRACT: We report a powerful and general concept for the design of three-dimensional metamaterials suitable for optically probed nanoscale sensing, combining the environmental sensitivity of localized surface plasmon resonances (LSPRs) and a low absorption of the probe light, even when the LSPRs are supported by lossy plasmonic elements. This concept is based on the tuning of the plasmon-induced Brewster conditions (angle of incidence and photon energy) of the material by suitable tailoring of its structure. This tuning is made possible by the interplay between LSPRs and optical interferences, i.e., the so-called plasmonic optical interferences. The plasmon-induced Brewster photon energy can be set outside the spectral range of the LSPR, thus in a spectral region of low optical absorption. Such “off-resonant” plasmon-induced Brewster conditions are exemplified in a self-assembled lamellar three-dimensional metamaterial consisting of stacked polymer layers doped with gold nanoparticles alternating with undoped polymer layers. At the “off-resonant” plasmon-induced Brewster conditions, an abrupt jump of the ellipsometric phase angle Δ occurs in the photon energy space. In the spectral vicinity of this jump, Δ shows strong sensitivity to the spectral features of the LSPR, potentially allowing the detection of infinitesimal LSPR energy shifts ($<10^{-5}$ eV) with a low absorptive loss of the probe light. The proposed concept has a wide outreach, as it can be applied regardless of the nature of the plasmonic element. It is appealing for the design of a broad variety of metamaterials (in terms of structure and composition) with multiple embedded sensing functionalities.

KEYWORDS: plasmonic optical interferences, 3D metamaterials, ellipsometry, nanoscale sensing, optical phase



The fast growth of plasmonics during the last decades has been largely sustained by the outstanding properties of plasmon resonances in assemblies of noble metal nanoparticles, such as spectrally sharp optical absorption and scattering features, nanoscale light confinement capability, and strong sensitivity to the nanoscale environment of the nanoparticles.¹ These properties have been mainly evidenced by the characterization and simulation of the effect of plasmonic systems on the intensity of light. In this context, nanoscale sensing has often been achieved by tracking, in optical transmittance or reflectance spectra, the energy shift of the plasmon resonances of assemblies of noble metal nanoparticles induced by changes in their nanoscale environment. This approach has allowed, for instance, the optical monitoring of biomolecule grafting on noble metal nanoparticles,² the selective sensing of gases trapped in a defective matrix encapsulating noble metal nanoparticles,³ or the optical measurement of the nanoscale distance between noble metal nanoparticles⁴ that can be useful for pressure monitoring. The potential of plasmonic nanoparticles for optically monitored nanoscale sensing goes beyond these few examples, in the context of the recently started quest aimed at fabricating plasmonic nanoparticles with an optical

response that could be tuned reversibly by an external excitation. Such “active” functionalities can be achieved in two different ways. The first one consists in embedding noble metal nanoparticles in an “active” shell/ultrathin layer with a reversibly tunable dielectric function. The second one consists in fabricating the plasmonic nanoparticles themselves from “active” elements, beyond noble metals. A broad variety of alternative plasmonic elements have been identified already,⁵ thus opening the way to a reversible tunability in the dielectric function of plasmonic nanoparticles through a wide range of external excitations (light, magnetic field, voltage, heat, etc.). Due to the reciprocity of transduction schemes, such reversible tunability in the nanoparticles’ optical response can be used for optically probed nanoscale sensing of the corresponding excitation.

The oscillatory electromagnetic fields of light are complex quantities described not only by their intensity but also by their phase. Upon interaction with an effective, nonmagnetic

Received: June 2, 2015

Published: September 15, 2015

medium, both the intensity and phase of an electromagnetic field are altered. This alteration is driven by the complex dielectric function $\varepsilon = \varepsilon_1 + j\varepsilon_2$ of the medium, ε_1 and ε_2 being linked by the Kramers–Kronig relations.^{5–7} In the case of a plasmonic effective medium, the dielectric function displays a spectral resonance that manifests itself by a bell-shaped variation of the ε_2 spectrum and an anomalous dispersion jump of ε_1 . These marked spectral variations can be used to drive in a controlled way the spectral features of an electromagnetic wave in both the intensity and phase spaces. This property has been used to design the so-called Huygens metasurfaces,⁸ which allow for instance driving the reflection and refraction angle of light away from the directions predicted by the classical Snell laws.⁹ These metasurfaces are efficient building blocks for the production of flat ultracompact photonic components.^{10,11} The effect of plasmon resonances on the phase of light has also been illustrated in several studies showing the spectroscopic ellipsometry analysis of planar assemblies of noble metal nanoparticles.^{6,12,13} Interestingly, it has been demonstrated^{13,14} that *tracking the ellipsometric phase angle* Δ in the spectral range of the plasmon resonances allows enhancing the sensitivity of nanoscale chemical sensing with respect to intensity tracking by conventional reflectance measurements. Important steps toward the development of ultrasensitive nanoscale sensors have been permitted by the demonstration of the plasmonic topological darkness phenomenon¹⁵ in planar ordered arrays of noble metal nanoparticles supporting collective plasmon modes. It provides the material with sharp plasmon-induced Brewster conditions (incident angle and photon energy), for which p-polarized light is not reflected ($|r_p| = 0$) and the ellipsometric intensity angle Ψ ($\tan \Psi = |r_p|/|r_s|$) drops to zero. At the plasmon-induced Brewster conditions, the ellipsometric phase angle Δ jumps abruptly of up to 180° in the photon energy space.^{15–17} Tracking of Δ in the spectral vicinity of the jumps has permitted unprecedentedly accurate gas¹⁵ or biological¹⁸ sensing in planar arrays of noble metal nanoparticles ordered and disordered on a substrate, respectively. In the latter case,¹⁸ the Δ jumps were related to a cancelation of r_s ($\Psi = 90^\circ$), induced by a Fano resonance resulting from the interplay between the localized surface plasmon resonance (LSPR) of the nanoparticles and the spectrally flat reflection at the substrate surface.^{19,20} Beyond these works that remain limited to two-dimensional assemblies of noble metal nanoparticles, topological darkness has recently been observed in three-dimensional metamaterials consisting of self-organized Ag@SiO₂ nanoparticles on a substrate.²¹ The observed plasmon-induced Brewster conditions originate in the combined occurrence of optical absorption and interferences. They can be predicted by computing the lines $|r_p| = 0$ for a given substrate and angle of incidence and looking for an intersection with the effective dispersion curve ($\varepsilon_1, \varepsilon_2, \lambda$) of the assembled material. At present, the tunability (in angle and photon energy) and potential for optically probed nanoscale sensing applications of plasmon-induced Brewster conditions in three-dimensional metamaterials remain to be experimentally and theoretically explored. This is especially true in the case of three-dimensional metamaterials that do not necessarily behave as an effective medium.

At present, integrated photonic applications demand the easy and large-scale fabrication of optical metamaterials operating in the near-UV–visible–near-IR spectral region, presenting *multiple embedded optically monitored sensing functionalities (beyond biological/chemical sensing)* and high optical throughput.²³

Three-dimensional plasmonic metamaterials²¹ are very interesting candidates in this context, due to their compatibility with chemical synthesis/self-assembly and physical deposition. These bottom-up fabrication methods allow building metamaterials from a broad compositional variety of plasmonic nanoparticles (beyond noble metals), embedding matrices, and ultrathin covering shells and layers, thus offering a wide spectrum of sensing functionalities. They allow a multiscale structuration of the metamaterial, suitable for combining optical effects related with the different scales (sub-nm, nm, μm). Especially, the size, shape, and three-dimensional organization of the nanoparticles can be controlled down to the scale of a few nanometers, suitable for tuning their plasmonic response and achieving effective optical properties (no relevant scattering of light) in the near-UV–visible–near-IR spectral region.

One important drawback of plasmonic metamaterials with regard to the high optical throughput requirement is the usually strong optical absorptive loss in the metal nanoparticles at the LSPR. This is particularly a problem in three-dimensional metamaterials, in which the optical path of the probe light is longer than in metasurfaces. This has prompted the development of low-loss plasmonic elements beyond the lossy metals (for instance transparent conductive oxides) to be used as building blocks of metamaterials.⁵ At present, the number of sensing functionalities available with low-loss plasmonic elements can in principle not compete with the broad choice offered by the lossy ones.

As an alternative to the search for the perfect lossless plasmonic element, we propose a powerful and general concept to achieve, by structural tailoring, valuable optically monitored LSPR-based nanoscale sensing functionalities with a low absorptive loss of the probe light in three-dimensional metamaterials *built from nanoparticles made of lossy plasmonic elements*.

This finding is based on a powerful and general concept: the tuning of plasmon-induced Brewster conditions in three-dimensional multiscale metamaterials due to the interplay between LSPRs and optical interferences (the so-called “plasmonic optical interferences”²⁴), both being highly tunable via the structure of the material. The plasmon-induced Brewster conditions can be driven in a broad angular and photon energy range. Especially, they can be tuned off-resonance (away from the LSPR photon energy, i.e., in spectral regions of low optical absorption). Under the “off-resonant” plasmon-induced Brewster conditions, an abrupt jump of the ellipsometric phase angle Δ occurs in the photon energy space. In the spectral vicinity of this jump, Δ shows strong sensitivity to the spectral features of the LSPR, while the probe light suffers a low absorptive loss.

We exemplify experimentally this genuinely original concept in the didactic case of three-dimensional multiscale lamellar plasmonic metamaterials synthesized using a facile method in self-assembled diblock copolymer templates. These metamaterials consist of a stack of alternated polymeric layers doped with noble metal nanoparticles and undoped polymer layers. The layer thicknesses and total thickness of the stack have been chosen (upon proper selection of the polymers) to be a few tens of nanometers and a few hundreds of nanometers, respectively. This ensures strong optical interferences in the stack. The concentration of metal nanoparticles in the doped polymer layers is controlled, allowing a broad range of tunability for their plasmonic response and thus for the plasmonic optical interferences in the whole lamellar metamaterial.

Then, we discuss the application of this concept for the development of three-dimensional metamaterials with multiple embedded optically monitored sensing functionalities (beyond chemical/biological sensing).

■ ACHIEVING PLASMON-INDUCED BREWSTER CONDITIONS USING PLASMONIC OPTICAL INTERFERENCES

Absorbing bulk materials behaving as an isotropic effective medium cannot display a Brewster angle, $|r_p|$ and Ψ never going to zero⁶ whatever the photon energy (E) and angle of incidence (AOI). This is exemplified in the case of a bulk effective medium with an LSPR-like absorption band, the dielectric function of which is plotted in Figure 1a (ϵ_{LSPR} dark gray

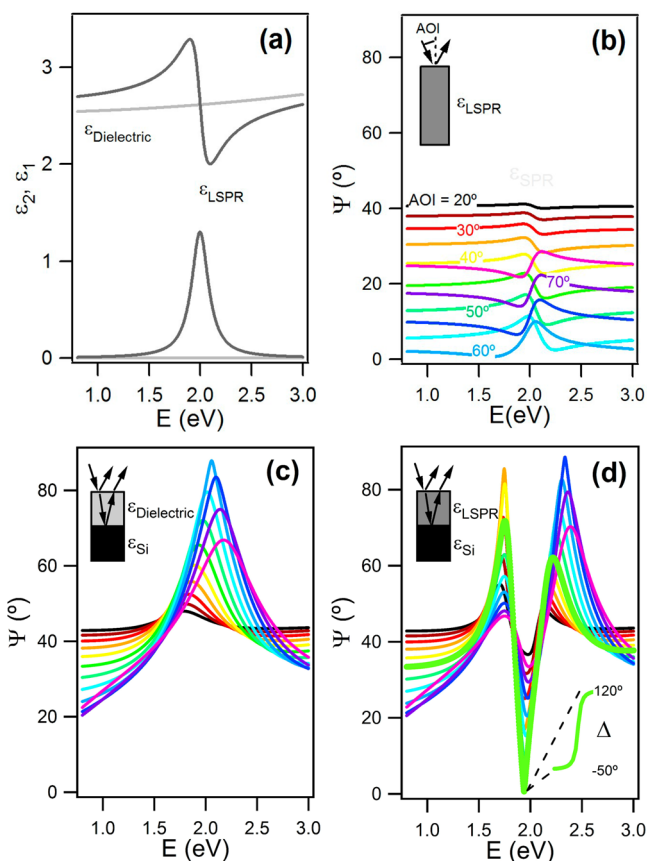


Figure 1. (a) Dielectric function ϵ (real and imaginary parts, ϵ_1 and ϵ_2) of a transparent dielectric material (“dielectric”) and a plasmonic effective medium presenting an LSPR signature typical of metal nanoparticles embedded in a dielectric medium (“LSPR”). Simulated Ψ spectra for different angles of incidence (multiples of 5°) of (b) a bulk plasmonic effective medium with dielectric function ϵ_{LSPR} shown in (a); (c) a 110 nm transparent thin film on bulk Si with dielectric function $\epsilon_{\text{dielectric}}$ shown in (a); (d) a 110 nm plasmonic thin film on bulk Si with dielectric function ϵ_{LSPR} shown in (a). In (b), (c), and (d), the same color scale has been used to compare the spectra at a given angle of incidence (AOI).

curves). The Ψ spectra of this medium are shown in Figure 1b. A variation of Ψ can be seen around the resonance energy (~ 2 eV), but Ψ never cancels. In contrast, for a fully transparent film on a reflecting substrate, zero $|r_p|$ values can be achieved at specific energies and angles of incidence. This is due to destructive optical interferences⁶ between the first reflection at the air/film interface and the coherent sum of the higher order

multiple reflections. In the case of semitransparent films on a metallic substrate, interferences can be used to generate optical blackbodies at specific incidence angle and photon energy^{25,26} depending on the nature of the film and substrate. In contrast with these, our work considers the possibility of achieving and using destructive interferences in films displaying an absorption band typical of the LSPR of nanoparticles embedded in a dielectric medium (such as the dielectric function ϵ_{LSPR} shown in Figure 1a).

This case is illustrated in Figure 1c and d. Figure 1c shows the Ψ spectra of a 110 nm transparent thin film (dielectric function $\epsilon_{\text{Dielectric}}$ light gray curve in Figure 1a) on a silicon substrate. These spectra present an interference-related, incidence-angle-dependent maximum around 2 eV. In contrast, the Ψ spectra for a film presenting a plasmon resonance (with a dielectric function being defined as $\epsilon_{\text{LSPR}} = \epsilon_{\text{Dielectric}} + \text{Kramers-Kronig consistent Lorentz oscillator}$; see details in section S1) show a sharp spectral hole around 1.94 eV, a zero Ψ value being obtained for an angle of incidence of 44.13° . In these angular conditions, a 180° Δ jump is achieved. This sharp spectral hole is due to the spectral modulation of the dielectric function of the medium introduced by the Lorentz oscillator, which makes the destructive interference conditions fulfilled in p-polarization.

This can be represented in three-dimensional space (ϵ_1 , ϵ_2 , λ), in which both the dispersion curve of the resonant material and the condition $|r_p| = 0$ for a given substrate and a given value of the angle of incidence appear as lines. The plasmon-induced Brewster condition occurs when such lines cross over. Such representation and further evidence of the fully destructive interference are given in section S1. Therefore, Brewster conditions can be achieved through the interplay between LSPRs and optical interferences in the film. This so-called “plasmonic optical interference”²⁴ phenomenon causes the topological darkness reported in the literature for metamaterials consisting of a three-dimensional self-organized assembly of Ag@SiO₂ nanoparticles.²¹ More importantly, the previous analysis provides physical concepts for the design of three-dimensional metamaterials in which the extensive tunability of the material structure will allow the control of plasmon-induced Brewster conditions together with efficient optically probed, LSPR-based nanoscale sensing solutions, as discussed in the following sections.

■ RESULTS

Synthesis of PS-Au Nanoparticles:P2VP Lamellar Metamaterials with Tunable Optical Interferences.

Polystyrene-*b*-poly(2-vinylpyridine) (PS-P2VP) copolymer films were first deposited on silicon wafers using spin-coating. Smooth, flat, and homogeneous films were obtained. Following deposition, the films were thermally annealed, which allowed the copolymers to self-assemble into a lamellar structure of alternating PS and P2VP layers. Au nanoparticles were then synthesized in situ within the films²⁷ following an infiltration process, in which the film-bearing wafer is dipped in a Au salt (HAuCl₄) solution and then in a reducing agent (NaBH₄) solution. Due to the strong affinity of P2VP to Au, Au nanoparticles form selectively in the P2VP layers, thus producing a structure of alternating PS and Au nanoparticles:P2VP nanocomposite layers. This infiltration procedure is repeated N times, and N controls the volume fraction of nanoparticles in the Au nanoparticles:P2VP layers.

Figure 2a shows the ellipsometric Ψ spectra for a PS-Au nanoparticles:P2VP lamellar metamaterial, as a function of the

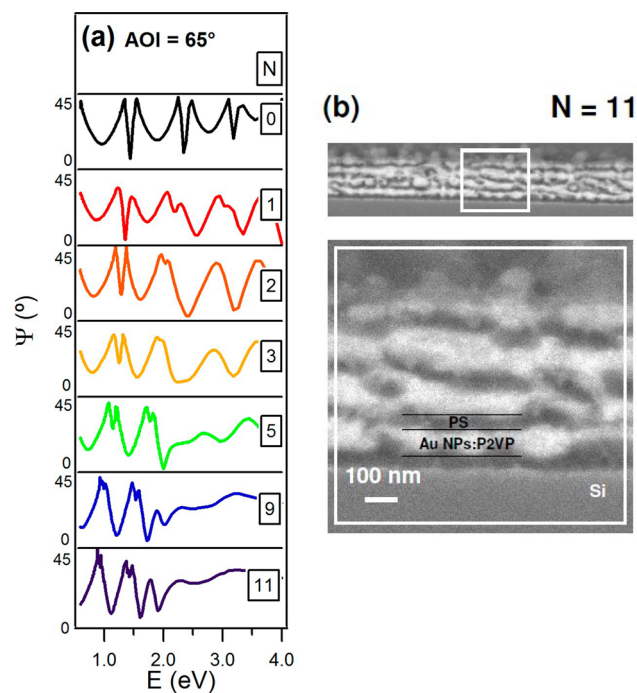


Figure 2. (a) Ellipsometric Ψ spectra at an angle of incidence of 65° for a PS-Au nanoparticles:P2VP lamellar metamaterial on a Si substrate after different numbers N of infiltration steps. The spectra are presented with vertical offsets for the sake of clarity. (b) Cross-section SEM micrograph of the metamaterial after $N = 11$ infiltration steps, and magnification of one part of the micrograph.

number N of infiltration steps. These spectra have been obtained at an angle of incidence of 65° and in the 0.6 to 4 eV photon energy range. Details about the ellipsometry setup and measurement are given in section S2. For the initial lamellar structure (i.e., before infiltration, $N = 0$), one can see periodic oscillations typical of interferences driven by reflections at the air/metamaterial and metamaterial/substrate interfaces, as both polymers are transparent in the studied energy range. At photon energies below ~ 1.6 eV, these interference features remain after successive infiltrations, suggesting that the metamaterial remains transparent in this range. Nevertheless, the extrema shift toward lower energies and their spectral separation decreases upon successive infiltrations, indicating an evolution possibly combining an increase in the total metamaterial thickness and a change in the effective dielectric function of the Au nanoparticles:P2VP layers. At photon energies above ~ 1.6 eV, interference fringes are still present, but their amplitude, width, and spectral separation change markedly after each infiltration. Up to $N = 2$, marked interference fringes remain. For $N = 3$, the interference fringes start to be damped. For $N > 5$, they have been rubbed out at photon energies above 2.2 eV. These effects are likely due to spectral changes in the effective dielectric function of the Au nanoparticles:P2VP layers as the volume fraction of Au increases and the strong absorption of light by the LSPR and interband transitions in Au nanoparticles become dominant. In these conditions, the incident light can be fully absorbed before it reaches the substrate, or reflections from the substrate can be fully absorbed before they reach the metamaterial surface. In

both cases, full absorption in the metamaterial prohibits any reflection coming from the metamaterial/substrate interface from interfering with the first reflection. These qualitative results show the strong tunability of optical interferences in the PS-Au nanoparticles:P2VP lamellar metamaterial in the whole studied photon energy range in relation with the nanoparticle formation. This tunability allows achieving sharp Ψ minima with a near-zero value for several different couples of angle of incidence and photon energy. This can be seen in Figure 2a (for instance for $N = 5$, $E \approx 1.95$ eV) and in section S3 (where the Ψ spectra obtained in a broad range of angles of incidence are shown). As Ψ depends sensitively on the angle of incidence, getting Ψ values as close as possible to zero first requires a more accurate angular scan than in the figures of section S3. An accurate determination of the optimum angles of incidence is done below in the paper.

Figure 2b shows a cross-section scanning electron microscope (SEM) image of the lamellar metamaterial after 11 infiltrations. It confirms the expected presence of Au nanoparticles:P2VP layers (bright regions) intercalated with PS layers (dark regions). The Au nanoparticles cannot be distinguished due to resolution limitation of the microscope. Although the interface of the Au nanoparticles:P2VP layers shows a roughness of tens of nanometers, it is worth noting that the layered structure is well defined over micrometric distances.

Plasmonic Optical Interferences for Nanoscale-Sensitive Off-Resonant Plasmonic Brewster Angles. In order to address the physical origin of the interferential structures shown in Figure 2a, a more complete optical characterization and analysis has been done on the PS-Au nanoparticles:P2VP lamellar metamaterial after 11 infiltrations. The ellipsometric spectra have been measured on this metamaterial in a broad range of angles of incidence (20° , 30° , 40° , 50° , 60° , 70°), in the 0.8 to 2.4 eV photon energy range. Moreover, the ellipsometric response of the metamaterial has been calculated at these six angles of incidence using the ellipsometric multilayer model shown in Figure 3a and fitted simultaneously to the six experimental spectra. This model was built to capture the main structural features of the lamellar metamaterial. It consists of intercalated effective medium layers (4) and dielectric layers (5), standing for the Au nanoparticles:P2VP layers and PS layers, respectively. The stack was completed by an effective surface roughness layer. More details about the ellipsometry setup, model, measurement, and fitting method are given in section S2. The best fit thicknesses, given in section S2, are consistent with the layer periodicity of the metamaterial as observed by SEM (Figure 2b). The best fit dielectric functions of the effective medium layers ($\epsilon_{\text{Effective medium}}$) and dielectric layers ($\epsilon_{\text{Dielectric}}$) are shown in Figure 3b. The experimental and best fit Ψ and Δ spectra are shown in Figure 3c, showing the good capability of the chosen model to account for all the interferential oscillations. As seen in Figure 3b, the imaginary part of $\epsilon_{\text{Effective medium}}$ presents a maximum at 2.15 eV (575 nm), while its real part displays an anomalous jump in the same spectral range. These features are typical of a resonant response, dominated by the LSPR of well-separated, spherical Au nanoparticles in a dielectric matrix. It is worth noting, as seen in Figure 3c, that the minima of Ψ occur at energies below 2 eV; that is, they never coincide with the maximum of the LSPR (occurring at $E_{\text{LSPR}} = 2.15$ eV).

Using the best fit ellipsometric model, simulations have been performed in order to predict the Brewster conditions of the

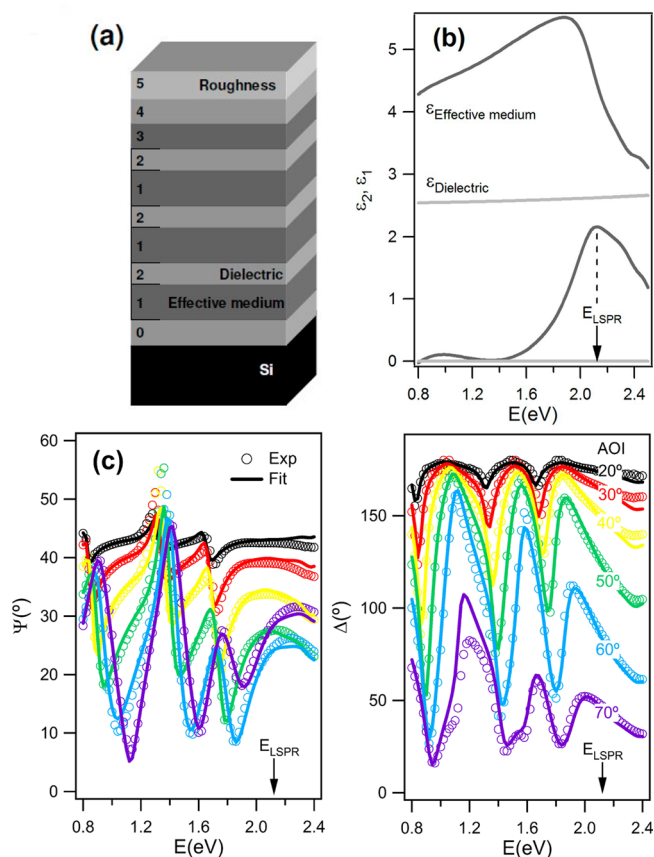


Figure 3. (a) Model used for fitting the ellipsometry spectra of a PS-Au nanoparticles:P2VP lamellar metamaterial with 11 infiltrations. (b) Best multiangle fit dielectric function of the dielectric layers ($\epsilon_{\text{Dielectric}}$; light gray curve) and effective medium layers ($\epsilon_{\text{Effective medium}}$; dark gray curve) using the ellipsometric model as shown in (a). (c) Ellipsometric angles (Ψ , left; Δ , right) of the lamellar metamaterial as experimentally measured (empty circles) and as given by the best multiangle fit (continuous lines) with the ellipsometric model shown in (a), for different values of the angle of incidence (as indicated on the right of the Δ plot). The best fit layer thicknesses are given in section S2.

lamellar metamaterial. As shown in Figure 4a, three sharp Ψ minima are predicted at energies of 1.13 eV (labeled “1”), 1.58 eV (“2”), and 1.83 eV (“3”), respectively, with a zero value at 1.13 and 1.58 eV. These theoretical predictions are corroborated by spectroscopic ellipsometry measurements (Figure 4a), which show three sharp minima superimposed with the calculated ones in the photon energy space. The experimental minima “1” and “2” are very close to 0 (a few tenths of a degree). The reasons for this nonexact experimental cancellation, together with the noncancellation of Ψ at minimum “3” in both experiment and simulations, are discussed in section S4, together with hints to achieve exact cancellations. Once again, it is worth noting that these minima are observed at energies different from that of the LSPR peak value ($E_{\text{LSPR}} = 2.15$ eV). These minima are observed at three different angles of incidence in the 55–71° range, with an agreement between theoretical calculations and experiment within 0.8–3.8°, which is a satisfactory result taking into account the simplicity of the ellipsometric model.

These sharp Brewster (“1” and “2”) and near-Brewster (“3”) conditions arise from destructive interferences of the p-polarized light upon interaction with the lamellar metamaterial, permitted by the particular values of the effective dielectric

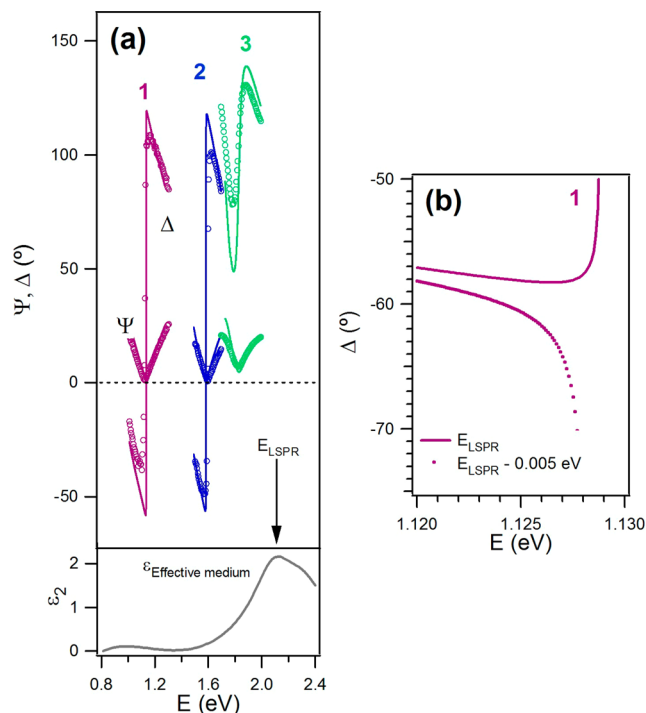


Figure 4. (a) Simulated (lines) and measured (open circles) Ψ and Δ spectra for a PS-Au nanoparticles:P2VP lamellar metamaterial after 11 infiltrations, limited to the spectral zones where plasmon-induced Brewster or near-Brewster conditions are fulfilled. The set of spectra labeled 1, 2, and 3 have been obtained at angles of incidence of 70.35°, 65.71°, and 56.40° by simulations and at angles of incidence of 66.5°, 64.9°, and 54.6° by measurements. (b) Simulated evolution of Δ values at the vicinity of the Δ jump upon 0.005 eV shift toward lower energy of the spectral features of the effective dielectric function $\epsilon_{\text{Effective medium}}$.

functions $\epsilon_{\text{Dielectric}}$ and $\epsilon_{\text{Effective medium}}$ at photon energies of 1.13, 1.58, and 1.83 eV. Further evidence of this interferential origin is given in section S4. The value of $\epsilon_{\text{Effective medium}}$ is relevantly dependent on the LSPR of the Au nanoparticles, even away from the photon energy of maximum LSPR absorption ($E_{\text{LSPR}} = 2.15$ eV). Indeed, as seen in Figure 3b, the real part of $\epsilon_{\text{Effective medium}}$ still presents a significant variation with energy down to 0.8 eV. This behavior is typical of Kramers–Kronig consistent oscillators and can also be seen in Figure 1a, where a very simple resonant system has been considered. Therefore, these Brewster or near-Brewster conditions are driven by the LSPR and can be obtained outside of the photon energy range of plasmonic absorption as seen in Figure 4a. They are thus “off-resonant” and occur in regions where the optical absorption is low. For instance, at 1.13 eV, the imaginary part of $\epsilon_{\text{Effective medium}}$ is as low as 0.07.

At these so-called off-resonant plasmon-induced Brewster or near-Brewster conditions, the ellipsometric phase angle Δ of the lamellar metamaterial shows abrupt jumps in the photon energy space, as seen in Figure 4a. Note that similar abrupt jumps are predicted for the same metamaterial structure when $|r_s| = 0$ (i.e., when $\Psi = 90^\circ$), as shown in section S4. Δ jumps upon cancellation of $|r_s|$ can be in principle broadly achieved with three-dimensional metamaterials and are conceptually equivalent to those achieved upon cancellation of $|r_p|$.

In the spectral vicinity of the jumps, Δ is strongly sensitive to small changes in the spectral features of the nanoparticles’ LSPR. This is illustrated in Figure 4b, which shows the

simulated effect on Δ at the vicinity of the 1.13 eV jump of a 0.005 eV shift toward lower photon energy (or a 1 nm red-shift) of the spectral features of the dielectric function $\epsilon_{\text{Effective medium}}$. Upon such shift, a Δ variation of several degrees is observed at fixed probe photon energy near the 1.13 eV jump. Assuming a linear dependence of the Δ value on the photon energy of the LSPR and an accuracy of 0.01° for the measurement of Δ (reached on last-generation well-calibrated ellipsometers), one predicts the possibility of detecting off-resonantly LSPR shifts of 10^{-5} eV. Further examples of this sensitivity are given in section S5 in the case of a pure Lorentzian resonance. Therefore, a tracking of Δ at a plasmon-induced Brewster angle and in the spectral vicinity of the corresponding off-resonant Δ jump potentially allows the detection of very small changes in the nanoscale environment or in the dielectric function of the Au nanoparticles embedded in the lamellar metamaterial, with a very low absorption of the probe light. The transduction mechanism is based on the measurement of changes in the effective dielectric function of the nanocomposite layers, the sensitivity being amplified by phase detection near the Δ jump. Upon shift of the LSPR toward lower photon energies and probing at a lower photon energy than the LSPR, the Δ change reflects an increase in the real part of the effective dielectric function of the nanocomposite layers.

Note that, in a real experiment, the LSPR shift is in general correlated with a change in the LSPR amplitude. For instance, an increase in the dielectric function of the nanoscale environment of spherical Au nanoparticles induces a shift of their LSPR toward lower photon energies, together with an increase in its amplitude.²⁸ These two correlated effects yield a stronger increase in the dielectric function of the nanocomposite layers than when considering the simplified case of an LSPR shift without change in amplitude. This means that, in adequate conditions, the sensitivity in a real experiment can be higher than in the simple case proposed above.

■ APPLICATIONS

Tunable Plasmon-Induced Brewster Conditions for Bulk Refractive Index Sensing. Upon optical phase monitoring in the vicinity of the Δ jumps, the simple lamellar metamaterial fabricated by a self-assembly method studied in this work can be used as a low-cost biological/chemical or gas sensor, with good bulk refractive index sensitivity. This sensitivity is studied in section S6. It is proposed that a value in the 10^{-6} RIU range can be achieved with a good monochromatic setup. It is comparable with the orders of magnitude found in the literature for LSPR-based detection: in the 10^{-6} RIU range for mixtures of liquids²⁹ and 10^{-5} RIU range for gases.² In contrast with these reports,^{2,29} no spectrum acquisition and spectral processing are needed. Although the record values achieved by SPR detection are not reached, we would like to stress that the easy and high tunability of the angle and photon energy of the plasmon-induced Brewster condition gives a better flexibility to fit with a given experimental setup than SPR systems in the Kretschman configuration.

Using Lossy Embedded Plasmonic Nanoparticles for Optically Monitored LSPR-Based Nanoscale Sensing with Low Absorptive Loss of the Probe Light. However, the main point of this paper is to provide hints for achieving efficient *nanoscale* sensing by *embedded* nanoparticles, in contrast with bulk refractive index sensing that involves the

effective response of the nanocomposite layers. It also goes beyond studying the particular sensitivity of the lamellar metamaterial consisting of Au nanoparticles embedded in a polymer matrix, which is not optimized nor designed on purpose for a specific sensing application.

From the results presented in the Results section (and depicted in Figure 4), we propose that accurate optically monitored LSPR-based sensing can be achieved with a *low absorptive loss* of the probe light, upon suitable structural tailoring and “off-resonant” probing, in three-dimensional metamaterials *built from nanoparticles made of lossy plasmonic elements*.

The proposed concept can be extended to the broad range of three-dimensional metamaterials (from the point of view of their composition and structure) that can be fabricated on purpose by chemical synthesis/self-assembly and physical deposition methods, with excellent optical quality in the near-UV–visible–near-IR spectral region. Abrupt “off-resonant” plasmon-induced Brewster Δ jumps can be achieved by plasmonic optical interferences and tuned in a broad angular and photon energy range by structural tailoring, *regardless the nature of the plasmonic element*.³⁰ The possibility to choose the desired plasmonic element (beyond noble metals or low-loss elements) opens the way to contactless probing of the physical variants (light, voltage, magnetic field, temperature, etc.) allowed by using *embedded* nanoparticles (as a directly “active” agent or through probing of their local environment: “active” ultrathin covering shell or layer). In contrast, we exclude a priori chemical/biological sensing that requires the nanoparticles to stand on top of a substrate. For instance, transitions in phase-change nanoparticles^{31,32} can be probed. In these cases, the reciprocity of transduction schemes makes the proposed concept suitable for the reversible tuning of the state of polarization of light.

The sensitivity of 10^{-5} eV (with monochromatic monitoring) to the LSPR photon energy estimated above is lower than the best values found in the literature (in the 10^{-5} eV², 10^{-6} eV,³³ and 10^{-7} eV³⁴ ranges, with spectral acquisition and processing). Better sensitivities can in principle be achieved in three-dimensional metamaterials by structural tailoring, for obtaining sharper resonances or locating the plasmon-induced Brewster conditions closer to the LSPR photon energy. However, we would like to stress that the first aim of this work is to show that a compromise can be achieved between losses and sensitivity (low losses and good sensitivity), by means of material design. Aiming at record sensitivities is beyond the scope of this paper.

Complex multiscale structures can be achieved easily with the vertical and lateral multiscale structuration capability (down to the nanoscale) offered by chemical synthesis/self-assembly and physical deposition methods.^{28,35,36} Especially, advanced lamellar configurations can be fabricated. They consist of several layers of functional nanoparticles with different size, shape, or composition, thus making possible the vertical integration of different sensing functionalities (sensitivity to different physical variants). We show in section S7 that a suitable vertical organization of the layers together with a suitable tailoring of their optical resonances and vertical localization make possible the individual optical phase tracking of their respective optical response. From this result, it is suggested that sensing with in-depth resolution or multivariant sensing can be achieved in advanced lamellar metamaterials without the need of spectral processing-based signal

deconvolution and without the need of unphysical statistical data analysis.³ This capability to embed vertically different functionalities may give a competitive advantage to three-dimensional lamellar metamaterials versus metasurfaces, since metasurface-based embedded multifunctionality relies mainly on a challenging lateral microscale integration of different metasurface components.

CONCLUSIONS

The potential of combining LSPRs and optical interferences has been reported in earlier works for tuning the intensity-related optical variants of simple metamaterials. This combination has been used to tailor their transmittance or reflectance spectra^{36–38} or to achieve enhanced plasmonic absorbance of the incident light.^{24,39} In the present work, we have demonstrated that these so-called plasmonic optical interferences open the way to achieving a much broader range of meta-optical effects. Especially, it has important consequences on the ellipsometric response of self-assembled three-dimensional PS-Au nanoparticles: P2VP lamellar metamaterials, which carries optical intensity and phase information (ellipsometric angles Ψ and Δ , respectively). We have shown that, due to plasmonic optical interferences in these metamaterials, plasmon-induced Brewster conditions ($\Psi = 0^\circ$) can be achieved at specific angles of incidence and at photon energies different from that of the LSPR (i.e., off-resonance). These angles and energies can be tailored by design of the metamaterial structure (nanoparticle volume fraction, layer thicknesses). Under illumination at any of these plasmon-induced Brewster angles, a phase jump is evidenced in the Δ spectrum around the zero- Ψ photon energy. At the spectral vicinity of this phase jump, Δ monitoring is expected to yield a good bulk refractive index sensitivity. In this context, the studied lamellar metamaterials can profit from their easy fabrication with high tunability in the plasmon-induced Brewster conditions.

At the spectral vicinity of the phase jump that can be driven in a spectral region of low optical absorption, Δ displays strong sensitivity to the LSPR photon energy, thus potentially allowing the detection of infinitesimal spectral shifts (10^{-5} eV) of the LSPR with a low absorptive loss of the probe light. This finding is particularly relevant for achieving, upon suitable structural tailoring, optically monitored LSPR-based nanoscale sensing with a low absorptive loss of the probe light in three-dimensional metamaterials built from embedded nanoparticles made of lossy plasmonic elements.

The possibility to choose the desired plasmonic element (“active” or “passive”, beyond noble metals or low-loss elements) and local environment (“active” or “passive” ultrathin covering shell or layer) opens the way to the design of metamaterial sensors suitable for probing many physical variants. The range of accessible physical variants can even be further extended, as nanoparticle resonances can also be achieved with polaritonic or excitonic elements.

On the basis of the excellent capability of chemical synthesis/self-assembly and physical deposition methods to fabricate advanced multiscale lamellar three-dimensional metamaterials with high optical quality, the easy and large-scale fabrication of high-throughput optically monitored multivariant sensors with a vertical integration of the different sensing functionalities seems possible. Such a configuration does not require a challenging lateral microscale integration of different components, which is a drawback of metasurface-based multivariant sensors. Moreover, it may allow to maximize the density of

functionalities on a board, in a similar way to 3D integration for electronics.⁴⁰

In summary, this work benefits the development of integrated nanoscale detection solutions based on three-dimensional metamaterials, combining the nanoscale environmental sensitivity of the resonances in nanoparticles built from the broad accessible range of “active” (even if lossy) elements, a low absorptive loss of the probe light inside the material, and the stability of optical phase monitoring. Although the concept presented here deals with lamellar metamaterials, it can be extended to more complex three-dimensional structures and also likely to metasurfaces in order to obtain a broader variety and tunability in the optical effects.

ASSOCIATED CONTENT

Supporting Information

The Supporting Information is available free of charge on the ACS Publications website at DOI: 10.1021/acsp Photonics.5b00306.

Interplay between LSPRs and optical interferences for achieving plasmon-induced Brewster conditions in a metamaterial (S1). Spectroscopic ellipsometry: experimental and analysis details (S2). Ellipsometry spectra of the lamellar metamaterial as a function of the number N of infiltration steps, at various angles of incidence (S3). Interplay between LSPRs and optical interferences for achieving plasmon-induced Brewster conditions in a lamellar metamaterial (S4). Sensitivity of Δ to the LSPR energy in off-resonant plasmon-induced Brewster conditions (S5). Tunable plasmon-induced Brewster conditions for bulk refractive index sensing (S6). Advanced lamellar configuration for multivariant sensing (S7) (PDF)

AUTHOR INFORMATION

Corresponding Author

*E-mail: johann.toudert@gmail.com.

Present Address

[§]Laser Processing Group, Instituto de Óptica, CSIC, Madrid, Spain.

Notes

The authors declare no competing financial interest.

ACKNOWLEDGMENTS

We thank A. Grigorenko, M. Warengem, K. Ehrhardt, and A. Baron for fruitful discussions, I. Ly for help in the electron microscopy characterization, and A. Turani-i-belloto for help in the data treatment. This work was supported by the LabEx AMADEus (ANR-10-LABX-42) in the framework of IdEx Bordeaux (ANR-10-IDEX-03-02).

REFERENCES

- (1) Maier, S. A. *Plasmonics, Fundamentals and Applications*; Springer: Berlin, 2007.
- (2) Bingham, J. M.; Anker, J. N.; Kreno, L. E.; Van Duyne, R. P. *Gas sensing with high-resolution localized surface plasmon resonance spectroscopy*. *J. Am. Chem. Soc.* **2010**, *132*, 17358–17359.
- (3) Joy, N. A.; Nandasiri, M. L.; Rogers, P. H.; Jiang, W.; Varga, T.; Kuchibhatla, V. N. T. S.; Thevuthasan, S.; Carpenter, M. A. Selective plasmonic gas sensing: H₂, NO₂ and CO spectral discrimination using a single Au-CeO₂ nanocomposite film. *Anal. Chem.* **2012**, *84*, 5025–5034.

- (4) Reinhard, B. M.; Siu, M.; Agarwal, H.; Alivisatos, A. P.; Liphardt, J. Calibration of dynamic molecular rulers based on plasmon coupling between gold nanoparticles. *Nano Lett.* **2005**, *5*, 2246–2252.
- (5) Naik, G. V.; Shalae, V.; Boltasseva, A. Alternative plasmonic materials: beyond gold and silver. *Adv. Mater.* **2013**, *25*, 3264–3294.
- (6) Fujiwara, H. *Spectroscopic Ellipsometry: Principles and Applications*; John Wiley & Sons, 2007.
- (7) Losurdo, M.; Hingerl, K. *Ellipsometry at the Nanoscale*; Springer: Berlin, 2013.
- (8) Yu, N.; Genevet, P.; Kats, M. A.; Aieta, F.; Tetienne, J. P.; Capasso, F.; Gaburro, Z. Light propagation with phase discontinuities: Generalized laws of reflection and refraction. *Science* **2011**, *334*, 333–337.
- (9) Aieta, F.; Genevet, P.; Yu, N.; Kats, M. A.; Gaburro, Z.; Capasso, F. Out-of-plane reflection and refraction of light by anisotropic optical antenna metasurfaces with phase discontinuities. *Nano Lett.* **2012**, *12*, 1702–1706.
- (10) Aieta, F.; Genevet, P.; Kats, M. A.; Yu, N.; Blanchard, R.; Gaburro, Z.; Capasso, F. Aberration-free ultrathin flat lenses and axicons at telecom wavelengths on plasmonic metasurfaces. *Nano Lett.* **2012**, *12*, 4932–4936.
- (11) Aieta, F.; Kats, M. A.; Genevet, P.; Capasso, F. Multiwavelength achromatic metasurfaces optical components by dispersive phase compensation. *Science* **2015**, *347*, 1342–1345.
- (12) Toudert, J.; Babonneau, D.; Simonot, L.; Camelio, S.; Girardeau, T. Quantitative modelling of the surface plasmon resonances of metal nanoclusters sandwiched between dielectric layers: the influence of nanocluster size, shape and organization. *Nanotechnology* **2008**, *19*, 125709–10.
- (13) Lodewijks, K.; Van Roy, W.; Borghs, G.; Lagae, L.; Van Dorpe, P. Boosting the figure of merit of LSPR-based refractive index sensing by phase-sensitive measurements. *Nano Lett.* **2012**, *12*, 1655–1659.
- (14) Grigorenko, A. N.; Nikitin, P. I.; Kabashin, A. V. Phase jumps and interferometric surface plasmon resonance imaging. *Appl. Phys. Lett.* **1999**, *75*, 3917–3919.
- (15) Kravets, V. G.; Schedin, F.; Jalil, R.; Britnell, L.; Gorbachev, R. V.; Ansell, D.; Thackray, B.; Novoselov, K. S.; Geim, A. K.; Kabashin, A. V.; Grigorenko, A. N. Singular phase nano-optics in plasmonic metamaterials for label-free single-molecule detection. *Nat. Mater.* **2013**, *12*, 304–309.
- (16) Huang, Y.; Ho, H. P.; Kong, S. K.; Kabashin, A. V. Phase-sensitive surface plasmon resonance biosensors: methodology, instrumentation and applications. *Ann. Phys.* **2012**, *524*, 637–662.
- (17) Vasic, B.; Gajic, R. Enhanced phase sensitivity of metamaterial absorbers near the point of darkness. *J. Appl. Phys.* **2014**, *116*, 023102.
- (18) Svedendahl, M.; Johansson, P.; Käll, M. Complete light annihilation in an ultrathin layer of gold nanoparticles. *Nano Lett.* **2013**, *13*, 3053–3058.
- (19) Svedendahl, M.; Käll, M. Fano interference between localized plasmons and interface reflections. *ACS Nano* **2012**, *6*, 7533–7539.
- (20) Svedendahl, M.; Verre, R.; Käll, M. Refractometric biosensing based on optical phase flips in sparse and short-range-ordered nanoplasmonic layers. *Light: Sci. Appl.* **2014**, *3*, e220.
- (21) Malassis, L.; Massé, P.; Tréguer-Delapierre, M.; Mornet, S.; Weisbecker, P.; Barois, P.; Simovski, C. R.; Kravets, V. G.; Grigorenko, A. N. Topological darkness in self-assembled plasmonic metamaterials. *Adv. Mater.* **2014**, *26*, 324–330.
- (22) Yang, Y.; Kravchenko, I. I.; Briggs, D. P.; Valentine, J. All-dielectric metasurface analogue of electromagnetically-induced transparency. *Nat. Commun.* **2014**, *5*, 5753.
- (23) Soukoulis, C. M.; Wegener, M. Past achievements and future challenges in the development of three-dimensional photonic metamaterials. *Nat. Photonics* **2011**, *5*, 523.
- (24) Choi, D.; Shin, C. K.; Yoon, D.; Chung, D. S.; Jin, Y. W.; Lee, L. P. Plasmonic Optical Interference. *Nano Lett.* **2014**, *14*, 3374–3381.
- (25) Kats, M.; Blanchard, R.; Genevet, P.; Capasso, F. Nanometre optical coatings based on strong interference effects in highly absorbing media. *Nat. Mater.* **2012**, *12*, 20–24.
- (26) Kats, A. M.; Sharma, D.; Lin, J.; Genevet, P.; Blanchard, R.; Yang, Z.; Qazilbash, M. M.; Basov, D. N.; Ramanathan, S.; Capasso, F. Ultrathin perfect absorber employing a tunable phase-change material. *Appl. Phys. Lett.* **2012**, *101*, 221101.
- (27) Sohn, B. H.; Seo, B. H. Fabrication of the multilayered nanostructure of alternating polymers and gold nanoparticles with thin films of self-assembling diblock copolymers. *Chem. Mater.* **2001**, *13*, 1752–1757.
- (28) Toudert, J. Modeling and optical characterization of the localized surface plasmon resonances of tailored metal nanoparticles. Kumar, C. S. S., Ed.; In *UV-VIS and Photoluminescence Spectroscopy for Nanomaterials Characterization*; Springer-Verlag: Berlin Heidelberg, 2013; pp 231–285.
- (29) Svedendahl, M.; Chen, S.; Dmitriev, A.; Käll, M. Refractometric sensing using propagating versus localized surface plasmons: a direct comparison. *Nano Lett.* **2009**, *9*, 4428–4433.
- (30) Toudert, J.; Serna, R.; *Polarization - Selective Optical Darkness in Metamaterials built from Nano-Bismuth*, META15 Conference, New York, 2015, Poster Communication 2P1-P7.
- (31) Toudert, J.; Serna, R. *Switchable Resonant Blackbody Metamaterials Based on Polaritonic Nano-Bismuth*, MRS, Spring, San Francisco, CA, 2015, Oral Communication Q2.02.
- (32) Jimenez de Castro, F.; Cabello, F.; Toudert, J.; Serna, R.; Haro-Poniatowski, E. Potential of bismuth nanoparticles embedded in a glass matrix for spectral-selective thermo-optical devices. *Appl. Phys. Lett.* **2014**, *105*, 113102.
- (33) Chen, S.; Svedendahl, M.; Käll, M.; Gunnarsson, L.; Dmitriev, A. Ultrahigh sensitivity made simple: nanoplasmonic label-free biosensing with an extremely low limit of detection for bacterial and cancer diagnostics. *Nanotechnology* **2009**, *20*, 434015.
- (34) Dahlin, A. B.; Tegenfeldt, J. O.; Höök, F. Improving the instrumental resolution of sensors based on localized surface plasmon resonance. *Anal. Chem.* **2006**, *78*, 4416–4423.
- (35) Toudert, J.; Serna, R.; López-Conesa, L.; Rebled, J. M.; Peiró, F.; Estradé, S.; Calvo-Barrio, L. Rare earth-ion/nanosilicon ultrathin layer: a versatile nanohybrid light-emitting building block for active optical metamaterials. *J. Phys. Chem. C* **2015**, *119*, 11800–11808.
- (36) Suárez-García, A.; Del Coso, R.; Serna, R.; Solís, J.; Afonso, C. N. Controlling the transmission at the surface plasmon resonance of nanocomposite thin films using photonic structures. *Appl. Phys. Lett.* **2003**, *83*, 1842–1844.
- (37) Garcia-Valenzuela, A.; Haro-Poniatowski, E.; Toudert, J.; Serna, R. Evolution of the optical reflectivity of a monolayer of nanoparticles during its growth on a dielectric thin film. *Appl. Phys. A: Mater. Sci. Process.* **2013**, *110*, 757–764.
- (38) Sannomiya, T.; Balmer, T. E.; Hafner, C.; Heuberger, C.; Vörös, J. Optical sensing and determination of complex reflection coefficients of plasmonic structures using transmission interferometric plasmonic sensor. *Rev. Sci. Instrum.* **2010**, *81*, 053102.
- (39) Zhang, N.; Liu, K.; Song, H.; Liu, Z.; Ji, D.; Zeng, X.; Jiang, S.; Gan, Q. Refractive index engineering of metal-dielectric nanocomposite thin films for optical super absorber. *Appl. Phys. Lett.* **2014**, *104*, 203112.
- (40) Materials challenges in 3D IC technology, MRS Bulletin 2015, Vol. 40, p 3.